September 2005

Thermally-actuated, phase change flow control for microfluidic systems

Zongyuan Chen
University of Pennsylvania

Jing Wang
University of Pennsylvania

Shizhi Qian
University of Pennsylvania

Haim H. Bau
University of Pennsylvania, bau@seas.upenn.edu

Thermally-actuated, phase change flow control for microfluidic systems

Abstract
An easy to implement, thermally-actuated, noninvasive method for flow control in microfluidic devices is described. This technique takes advantage of the phase change of the working liquid itself—the freezing and melting of a portion of a liquid slug—to noninvasively close and open flow passages (referred to as a phase change valve). The valve was designed for use in a miniature diagnostic system for detecting pathogens in oral fluids at the point of care. The paper describes the modeling, construction, and characteristics of the valve. The experimental results favorably agree with theoretical predictions. In addition, the paper demonstrates the use of the phase change valves for flow control, sample metering and distribution into multiple analysis paths, sealing of a polymerase chain reaction (PCR) chamber, and sample introduction into and withdrawal from a closed loop. The phase change valve is electronically addressable, does not require any moving parts, introduces only minimal dead volume, is leakage and contamination free, and is biocompatible.

 Reprinted from the *Lab on a Chip*, Volume 5, Issue 11, September 21, 2005, pages 1277-1285.

Thermally-actuated, phase change flow control for microfluidic systems†

Zongyuan Chen, Jing Wang, Shizhi Qian and Haim H. Bau*

Received 10th June 2005, Accepted 26th August 2005
First published as an Advance Article on the web 21st September 2005
DOI: 10.1039/b508275g

An easy to implement, thermally-actuated, noninvasive method for flow control in microfluidic devices is described. This technique takes advantage of the phase change of the working liquid itself—the freezing and melting of a portion of a liquid slug—to noninvasively close and open flow passages (referred to as a phase change valve). The valve was designed for use in a miniature diagnostic system for detecting pathogens in oral fluids at the point of care. The paper describes the modeling, construction, and characteristics of the valve. The experimental results favorably agree with theoretical predictions. In addition, the paper demonstrates the use of the phase change valves for flow control, sample metering and distribution into multiple analysis paths, sealing of a polymerase chain reaction (PCR) chamber, and sample introduction into and withdrawal from a closed loop. The phase change valve is electronically addressable, does not require any moving parts, introduces only minimal dead volume, is leakage and contamination free, and is biocompatible.

1. Introduction

Flow control in integrated, multifunctional microfluidic devices remains a major challenge. Often the flow control is accomplished with the use of valves. Some of the concerns associated with microvalves are dead volume, leakage, contamination, biocompatibility, the timing of the actuation, fabrication complexity, cost, and performance. These issues are particularly acute in the case of disposable devices when cost considerations are paramount. Not surprisingly, a considerable effort has been invested in the development of microvalves.[1–18] While many of these microvalves are miniaturized versions of their macro, conventional counterparts, some of them are based on unconventional concepts ranging from elastomer,[9,10] hydrogel,[11,12] paraffin,[13,14] and ice valves[15–18] to colloid valves manipulated by magnetic[8] and electromagnetic[7] fields.

Although these innovative valves offer many advantages, they also suffer from several shortcomings. With the exception of the hydrogel and ice valves, all the other valves require a sensor to time the closing of the valve. Elastomer valves require either a mechanical or a hydraulic system to provide the necessary actuation forces. Hydrogel and wax/paraffin valves, when in direct contact with the working liquid, introduce foreign materials into the conduits, raising concerns of contamination and biocompatibility. Moreover, hydrogels may absorb proteins and enzymes, depleting the sample of valuable reagents. The wax/paraffin valves are the closest in concept to the ice valves that we describe in this paper and have the advantage of being normally closed at room temperature. Unfortunately, it is difficult to position the molten paraffin/wax at the desired locations needed to achieve appropriate sealing. Nevertheless, Liu *et al.*[13] and Pal *et al.*[14] demonstrated, respectively, integrated microfluidic systems operating with ''one-shot'' paraffin valves and reusable paraffin valves with special conduit designs.

Bevan and Mutton[15] proposed an interesting alternative and demonstrated the freezing of a liquid slug in stainless steel and fused silica tubes with liquid carbon dioxide spray. More recently, He *et al.*[16] demonstrated the feasibility of freeze–thaw in a fused-silica capillary cooled by a thermoelectric unit, and Liu and Gui[17] repeated the test with a stainless steel tube.

We used the phase change (PC) valve for the control of the flow in a disposable, polycarbonate cassette designed for the identification of pathogens in samples of oral fluids at a point of care facility.[18] The cassette consists of multiple analysis paths that necessitate sample metering, distribution, and flow control. Since the cassette is intended to be disposable, simplicity and cost are of great importance. The cassette is designed to operate with external chemistry and analysis boxes for the supply of power, reagents, and optical detection. Thus, in contrast to stand-alone devices, our device is not constrained by stringent power consumption limitations.

The PC valve has many advantages. It is noninvasive, simple to construct and operate, provides a perfect seal, can withstand very high pressures without fail, and does not introduce any foreign materials into the system. There are no positioning problems such as with the wax/paraffin valves. Moreover, in certain cases, the valve can operate in a self-actuated mode, alleviating the need for a sensor to determine the appropriate actuation time. For example, when a liquid slug is driven into a cassette, a precooled conduit section would allow the free passage of air prior to the arrival of the liquid slug and would seal at the desired time when the slug arrives at the valve location. The disadvantages of the PC valve include relatively

Department of Mechanical Engineering and Applied Mechanics, University of Pennsylvania, Philadelphia, PA 19104-6315, USA. E-mail: bau@seas.upenn.edu

† Electronic supplementary information (ESI) available: videoclips of sample distribution and metering and of filling and emptying a closed loop; and a discussion of the temperature of the thermoelectric unit in contact with the chip and convective heat transfer coefficient. See http://dx.doi.org/10.1039/b508275g

high-energy consumption, relatively slow response, and a normally open state.

The manuscript is organized as follows. Section 2 describes the design and fabrication of the PC valve and the experimental set-up. Section 3 describes the characterization of the PC valve. Section 4 presents a computational model of the phase change valve and compares the theoretical predictions with experimental observations. Section 5 describes the use of the valve for various tasks in a microfluidic system such as sample metering and distribution, sealing the PCR chamber, and filling and emptying a closed-loop reactor.

2. Design and fabrication of the PC valve and the experimental set-up

The PC valve consists of a microconduit and a thermoelectric unit in thermal contact with the microconduit. A small section of the conduit is cooled well below the freezing point of water. When the conduit contains liquid, a segment of the liquid freezes and blocks the passage. This is the closed state of the valve. To re-open the valve, the thermoelectric unit is turned off, and the ice is allowed to thaw. If desired, the thawing time can be shortened by actively heating the ice with the thermoelectric unit or with a resistor heater.

A microconduit with a rectangular cross-section (width × height) of 250 μm × 180 μm was fabricated with a computer-controlled (CNC) milling machine (Fadal, Chatsworth, CA) in 770 μm thick polycarbonate (Ensinger). The sheet containing the conduit was thermally bonded with a second 250 μm thick polycarbonate sheet to form a capped conduit. The bonding was accomplished by laminating both sheets for 60 minutes at 143 °C under 180 kg of force over the top and bottom surfaces of the chip (49.3 mm × 13.6 mm) with a press (Carver Inc., Wabash, IN). The thermal bonding process caused slight changes in the dimensions of the conduit. Subsequent to the bonding process, the conduit dimensions measured (width × depth) 233 μm × 172 μm and the total thickness of the chip became 950 μm. These dimensional changes can be compensated for by appropriate design.

Fig. 1 depicts schematically the experimental apparatus used for the characterization of the PC valve. Teflon tubing (inner diameter 764 μm, DABURN Electronics & Cable Corp., NJ) connected the syringe pump (kd Scientific, PA) to the inlet of the conduit. The conduit outlet was connected with a Teflon tube to a drain. A type-K thermocouple (Omega, each wire was 75 μm in diameter and the junction diameter was ~170 μm) was inserted through the side of the chip so that the center of the junction was adjacent to the sidewall of the conduit and located at the midheight of the conduit, at a distance of ~15 μm from the surface of the side wall. The polycarbonate device was placed on the top of a thermoelectric (TE) unit (10.3 mm × 6.2 mm, Melcor Corp., Trenton, NJ) with the nominally 250 μm thick conduit cover being in contact with the TE. The length of the TE was parallel to the conduit. The TE unit was mounted on top of a heat sink equipped with a fan. Thermal, 7–11 μm thick grease was applied at the interface between the polycarbonate and the TE and at the interface between the TE and the heat sink to reduce the thermal contact resistance. The thermocouple was connected to a HP 3458A multimeter *via* a 20-channel relay multiplexer with electronic zero (HP 3852A). An HP 6621A power supply provided DC power to the thermoelectric unit. The HP units were controlled by a computer *via* a PCI-GPIB interface. The control algorithm was programmed with LabVIEW™ (National Instruments, Austin, TX).

3. Characterization of the PC valve

In this section, we describe the operation of the valve and characterize its performance under various operating conditions. The characterization of the valve was experimentally conducted by measuring its response time as a function of power consumption, pressure head (flow rate), and precooling duration. The results have been used as a design guide for our specific valve applications, and they point to ways in which the valve can be modified to improve its performance.

We used the PC valve in two different modes of operation. In the first mode, the thermoelectric unit was turned on when

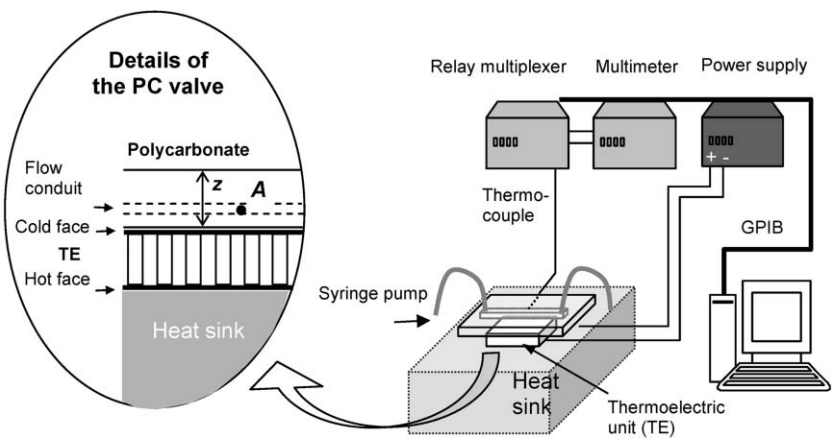

Fig. 1 A schematic depiction of the experimental apparatus for the characterization of the PC valve. The dimensions of the flow conduit are: 233 μm × 172 μm × 38.2 mm (width × depth × length). The polycarbonate chip thickness z is 950 μm. The distance between the bottom of the conduit and the surface of the polycarbonate that is in contact with the thermoelectric unit (TE) is 250 μm. Label ***A*** indicates the thermocouple tip located at the center of the microconduit side wall above the center of the thermoelectric unit.

the valve section of the conduit was filled with liquid. In this case, the response time (t_A) was defined as the time elapsing between the turning on of the thermoelectric unit and blockage of the conduit. This time consists of the time required to cool the TE unit and the polycarbonate substrate as well as the time needed to freeze the liquid. In the second mode of operation, the valve segment of the conduit was precooled prior to the arrival of the liquid slug, and the response time (t_B) was defined as the time elapsing between the instant of the arrival of the liquid slug at the valve location and the blockage of the conduit. Clearly, $t_B < t_A$.

The first set of tests was conducted under static conditions in the absence of flow. The conduit was filled with water, and the water was kept stagnant. Fig. 2 depicts the temperature at the center of the conduit as a function of time for various levels of power applied to the TE unit: 1.7, 2.0, 2.6, 3.3, 5.9 and 6.9 W. The time zero corresponds to the instant when the power to the TE was turned on. Initially, the temperature decreased as the time increased. The freezing of the liquid is indicated by a temperature jump resulting from the release of the latent heat during the ice formation. The ice formed when the temperature at the location of the thermocouple fell below −17 °C. The freezing process occurred during the ascending part of the temperature jump, and it was completed within less than 60 ms (the time resolution of our data acquisition system). Close inspection under a microscope revealed that the freezing process occurred very rapidly. In addition to the microscope observations, this assertion was supported by simultaneous multi-point temperature recordings—all of which recorded temperature jumps at about the same time. The supercooling temperature is likely to depend on a number of factors such as the availability of nucleation sites, the rate of cooling, and surface conditions.

Fig. 3 depicts the response time as a function of the power input to the TE unit. The symbols and the solid line correspond, respectively, to experimental data and theoretical predictions. The mathematical model that was used to calculate the theoretical predictions is described later in the paper. The response time decreased as the power input to the TE unit increased. Increasing the power input above ~4.5 W resulted, however, in diminishing returns. In the absence of flow, the asymptotic value of the time delay was about 6 seconds. This time delay was caused by the thermal inertia of the TE unit and the polycarbonate, substrate material. The time constant of the TE unit was estimated by applying a step change in the power input to the TE unit and measuring the temperature of the polycarbonate–TE unit interface as a function of time. The times needed for the surface of the TE to cool from room temperature to −17 °C were, respectively, 3.2, 4, and 8 s when the power levels were 6.9, 3.7 and 1.8 W. The time constant of the polycarbonate is estimated as $\tau^s \sim \rho^s C_p^s H^2/k^s \sim 0.5$ s, where $\rho^s = 1300$ kg m^{-3} is the density (measured in-house), $C_p^s = 1200$ J kg^{-1} K^{-1} is the specific heat, $k^s = 0.21$ W m^{-1} K^{-1} is the thermal conductivity,[19] and $H = 250$ μm is the distance from the conduit bottom to the TE surface. In the above, the superscript (s) denotes the polycarbonate substrate. The response time is dominated by the time constant of the TE unit.

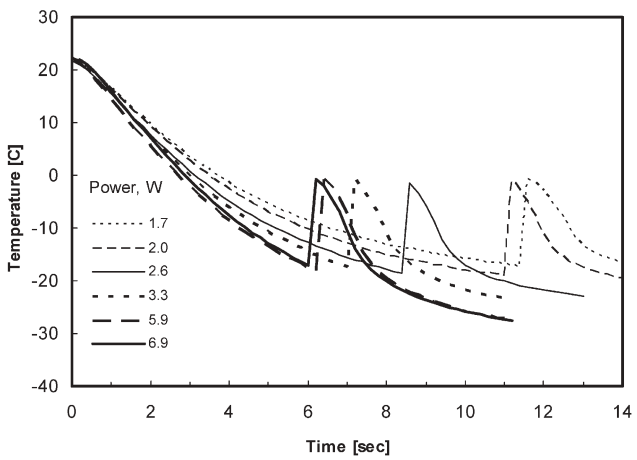

Fig. 2 The temperature at the center of the conduit is depicted as a function of time. The conduit is filled with stationary water. The various curves correspond to different levels of power, 1.7, 2.0, 2.6, 3.3, 5.9, and 6.9 W, supplied to the thermoelectric unit. The thermoelectric unit was turned on at time zero.

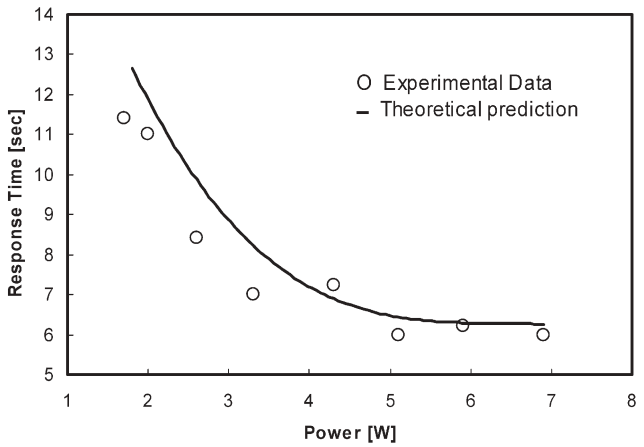

Fig. 3 The response time of the PC valve is depicted as a function of the power supplied to the TE unit in the absence of flow. The circles and line correspond, respectively, to experimental data and theoretical predictions.

Similar measurements to the ones depicted in Fig. 2 were carried out in the presence of fluid flow. Once a certain flow rate was established, the time elapsing between the turning on of the thermoelectric unit and the cessation of the flow was recorded. Fig. 4 depicts the response time as a function of the flow rate. The symbols and the solid line correspond, respectively, to experimental data and theoretical predictions. When the flow rate was smaller than 30 μL min^{-1}, the response time increased slowly from 5.6 to 9 s as the flow rate increased. When the flow rate exceeded 30 μL min^{-1}, the response time increased much faster as the flow rate further increased. Once the flow rate reached 46 μL min^{-1}, freezing no longer occurred. This threshold is likely to increase as power supply to the thermoelectric unit is increased and/or ice nucleation is enhanced.

We estimate the order of magnitude of the maximum Peclet number (Pe_{max}) at which freezing will no longer occur by comparing the thermal (diffusion) penetration time through

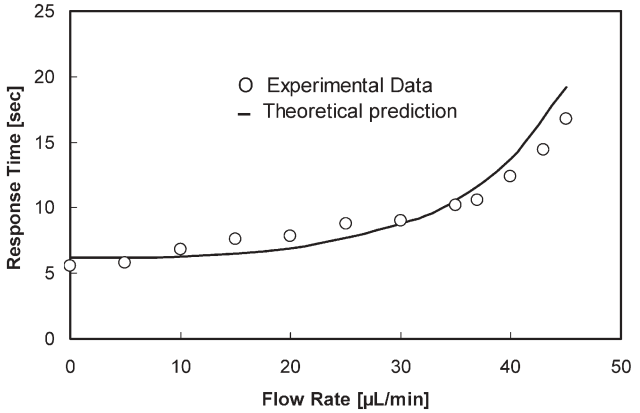

Fig. 4 The response time of the PC valve is depicted as a function of the flow rate. The circles and the solid line correspond, respectively, to experimental data and theoretical predictions. The power input to the TE is 6.9 W.

the height of the conduit (S) with the residence (advection) time of the fluid in the cooled section. $Pe_{\max} = \frac{v_{\max} S}{\alpha^w} \sim \frac{L}{S}$, where L is the length of the cooled section, $v_{\max}$ is the cross-sectional average fluid velocity, and α^w is the thermal diffusivity of the fluid. This estimate yields $Pe_{\max} \sim 60$. In the experiment, we find that $Pe_{\max} > 24$.

An interesting feature of the PC valve is its ability to operate in a self-actuated mode. A small section of the conduit is precooled to a temperature well below the freezing temperature of the fluid. When a liquid slug is upstream of the cooled section, the valve allows free passage of air, but when the front of the liquid slug arrives at the "valve" location, the liquid freezes and blocks the passage. Fig. 5 depicts the response time of the valve as a function of the precooling time when the power supply to the thermoelectric unit was 3.3 W and the pressure head was 5.7 kPa. At room temperature, this pressure head corresponded to a flow rate of 118 μL min^{-1}. Once cooling started, the liquid viscosity increased and the flow rate decreased. The symbols in Fig. 5 correspond to experimental data, and the solid line was added for clarity. The response time is defined as the time elapsing between the arrival of the liquid slug at the valve location and the blockage of the conduit. The precooling time is defined as the time interval between the turning on of the thermoelectric unit and the instant when the flow was turned on. When the precooling times were less than 6 s, the response time was 8.7 s and was independent of the precooling time. When the precooling time was between 6 and 12 seconds, the response time decreased as the precooling time increased. When the precooling time was larger than 12 s, the response time was about 0.5 s and nearly independent of the precooling time. Further increases in the precooling time did not have any effect. The 0.5 s response time is dictated by the mass of the liquid in the cooling section and the effectiveness of the heat transfer process.

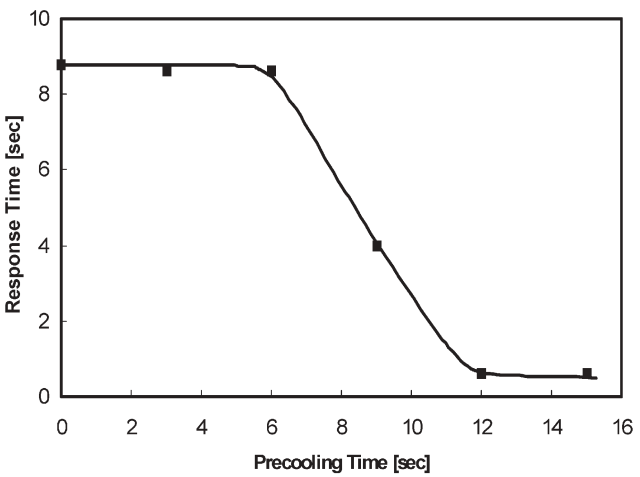

Fig. 5 The response time of the precooled PC valve is depicted as a function of the precooling time. The TE power is 3.3 W and the flow rate (in the absence of cooling) is 118 μL min^{-1}.

Next, we examine the time constant associated with the opening of the valve. In order to open the valve, the ice needs to melt. In our experiments, we relied on the heat interaction with the ambient to provide the necessary energy to thaw the ice. This process lasted about 6 seconds. This time constant can be shortened, however, by reversing the polarity of the thermoelectric unit so that it operates as a heat pump or by installing and activating a resistance heater in close proximity to the valve location.

Finally, another characteristic of interest is the amount of pressure that the valve can withstand without allowing any liquid flow (leakage). To estimate the holding capacity of the valve, we froze a liquid slug and applied air pressure upstream with a gas-tight syringe pump. The pressure was estimated by monitoring the volume of the air pocket trapped between the liquid and the pump piston. The pressure of the compressed air was increased up to 360 kPa without any evidence of leakage. Thus, the holding pressure of the valve is at least 360 kPa and likely much higher.

The valve described above was not optimized with respect to its response time. The response time can be reduced by reducing the response time of the TE and by reducing the thermal inertia and increasing the thermal conductivity of the substrate material. In order to study these various effects on valve performance, we constructed a mathematical model, which we describe in the next section.

4. Mathematical model

In this section, we study the temperature distribution in the polycarbonate substrate and in the fluid using a three-dimensional model that accounts for heat conduction in the polycarbonate and convection in the conduit. The theoretical predictions are compared with the experimental data. The simulations also allow us to examine the effects of various factors on valve performance.

The computational domain is depicted in Fig. 6. Fig. 6a and 6b depict, respectively, cross-sections of the device that are parallel and transverse to the flow direction. The various geometrical dimensions are indicated in the figures (in mm). In some of our simulations, we investigated the effect of an air gap located above the conduit on the performance of the valve. For this reason, although there was no air gap in our

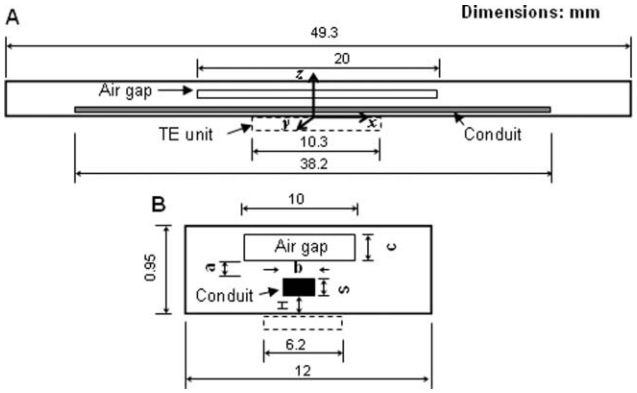

Fig. 6 Cross-sections of the device that are parallel (**A**) and transverse (**B**) to the flow direction. The dashed rectangle represents the TE unit. All dimensions are in mm. The drawing is not to scale. a = 0.1 mm, b = 0.233 mm, c = 0.377 mm, S = 0.172 mm, and H = 0.25 mm.

experimental set-up, the air gap is depicted in the various cross-sections in Fig. 6.

We consider an incompressible liquid. The energy equations in the fluid and solid are, respectively,

$$\rho^{w} C_p^{w} \left(\frac{\partial T}{\partial t} + \vec{u} \bullet \nabla T \right) = k^{w} \nabla^2 T \tag{1}$$

and

$$\rho^{s} C_p^{s} \frac{\partial T}{\partial t} = k^{s} \nabla^2 T \tag{2}$$

In the above, $\vec{u}(x,y,z)$ is the velocity vector. $T(x,y,z)$, ρ, C_p, and k are, respectively, the temperature, density, specific heat at constant pressure, and thermal conductivity. Superscript w denotes water. All properties are assumed temperature-independent, and their values are taken at room temperature 25 °C. In order to carry out the simulations with limited computer resources, we used in our simulations the velocity profile of fully-developed flow in a rectangular cross-section for which an analytic expression is available.[20]

On the outer surface of the substrate, we specified the Robins boundary condition:

$$-k^{s} \nabla T \bullet \vec{n} = h_a (T - T_\infty) \tag{3}$$

where $\vec{n}$ is the outward unit vector normal to the surface; h_a is the convective heat transfer coefficient between the substrate surface and the environment, and T_∞ = 298 K is the ambient temperature. The convective heat transfer coefficient h_a = 47.5 W m^{-2} K^{-1} was estimated by solving an inverse problem to match the experimental data with model predictions (see Electronic Supplementary Information†). When the air gap was included in the simulations, we specified the thermophysical properties of air for the material in the gap and we assumed stationary air.

For lack of an appropriate time-dependent model for the thermoelectric unit, we carried out a sequence of measurements to determine the temperature of the thermoelectric unit–polycarbonate interface as a function of time and power supplied to the thermoelectric unit. The time was measured from the instant when the thermoelectric unit was turned on. In other words, the thermoelectric unit was subjected to a step change in power. The hot face was in contact with a heat sink equipped with a fan. The temperature of the TE–polycarbonate interface T_i (K) correlated within ±1 °C with the expression:

$$T_i = 298 - \left\{ 27 + 44 \exp\left[-\frac{1}{0.7(P+0.4)} \right] \right\} \exp\left[-\frac{1}{0.7(t+0.4)} \right] \tag{4}$$

where 298 K is the room temperature, P is the power (W) input to the TE unit, and t is time (s). For a comparison of the predictions of eqn (4) with experimental data, see Electronic Supplementary Information†. Eqn (4) served as a temperature boundary condition in our simulations.

At the interface between the solid wall and the fluid, we satisfy, respectively, temperature

$$T^{s} = T^{w} \tag{5}$$

and flux

$$-k^{s} \nabla T^{s} = -k^{w} \nabla T^{w} \tag{6}$$

continuities.

The temperature of the fluid at the inlet cross-section is assumed uniform and equal to the ambient temperature

$$T = T_\infty \tag{7}$$

At the exit of the conduit, the total flux is dominated by the convective flux and the normal conductive flux

$$-k^{w} \nabla T^{w} \bullet \vec{n} = 0 \tag{8}$$

In our simulations, we used ρ^{w} = 1000 kg m^{-3}, C_p^{w} = 4180 J kg^{-1} K^{-1}, and k^{w} = 0.61 W m^{-1} K^{-1}. The thermophysical properties of the polycarbonate were specified earlier in the paper.

The three-dimensional model was solved with the finite element package FEMLAB‡. We used non-uniform elements, with a finer mesh in the region of the flow conduit. We verified that for the conditions studied here, the numerical solutions were convergent and independent of the sizes of the element, and the results of the calculations satisfied the various conservation laws.

Initially, the simulations were carried out for the geometry and thermal conditions of the experimental set-up (Fig. 6 without the air gap). We computed the temperature at the thermocouple location as a function of time prior to the ice formation. Since the experimental observations indicated that the ice formed nearly instantaneously once the temperature reached a certain supercooling value T_{ice}, we associated ice formation and valve closing with the instant when the computed temperature reached T_{ice} = −17 °C, which is the temperature at which ice formation was observed in our experiments.

‡ FEMLAB is a product of COMSOL Inc., Sweden (http://www.femlab.com).

Fig. 3 and 4 depict, respectively, the theoretical predictions (solid lines) for the valve response time as a function of the thermoelectric unit power supply in the absence of flow and the response time as a function of the flow rate when the power is 6.9 W. In both cases, the theoretical predictions are in good agreement with experimental data. The ability of the model to reproduce experimental observations provides us with the confidence that the code can be used as a design and optimization tool.

Next, we estimated the size of the region that is affected by the TE. Fig. 7 depicts the steady state temperature distribution (color-coded) and contours of $\phi = \left(\frac{T_\infty - T(t)}{T_\infty - T_i(t)}\right)$ in the cross-section of the device that is transverse to the conduit and located at the mid-length of the TE. In the above, $T_i(t) \sim 243$ K is the temperature of the TE–polycarbonate interface. The figure is not drawn to scale, and the vertical coordinate is stretched. The power input to the TE unit is 6.9 W, and there is no flow. The distance from the edge of the TE to the contour line $\phi = 0.04$, where the temperature $T(t)$ is 2.2 °C lower than the ambient temperature, is about 2.9 mm. This distance defines the range of influence of the TE unit. The "influence" distance can be reduced by introducing air gaps into the substrate.

Finally, we investigate briefly two possible design improvements. In case I, we consider the effects of an air gap of height $c = 0.377$ mm located above the conduit and a reduced distance (H) between the conduit and the surface of the TE. In case II, we examine the effect of reducing the footprint of the thermoelectric unit with the objective of reducing the power consumption of the unit and the cooled volume of the substrate.

Fig. 8 depicts the estimated response time in the absence of flow as a function of the power input to the TE. The dashed, heavy solid, and light solid lines correspond, respectively, to the base case (for which we carried out the experimental work), case I, and case II. In case I, the air gap reduces the thermal interaction between the valve region and the ambient. An air gap of dimensions $L \times W \times H = 20$ mm $\times$ 10 mm $\times$ 377 μm is cut in the polycarbonate 100 μm above the conduit (Fig. 6). Additionally, the distance H between the bottom of the conduit and the surface of the TE is reduced to 150 μm. The air in the gap is stationary. When the TE power level is 6.9 W, in the base case, the response time for ice formation is 6.2 s. The reduction of H alone improves the time constant to 5.1 s. The air gap alone reduces the time constant to 4.9 s. The reduction in H combined with the air gap reduces the response time to 4.1 s. Given the fact that response time is dominated by the thermal inertia of the TE unit, it is not surprising that the effects of the design modifications are relatively modest.

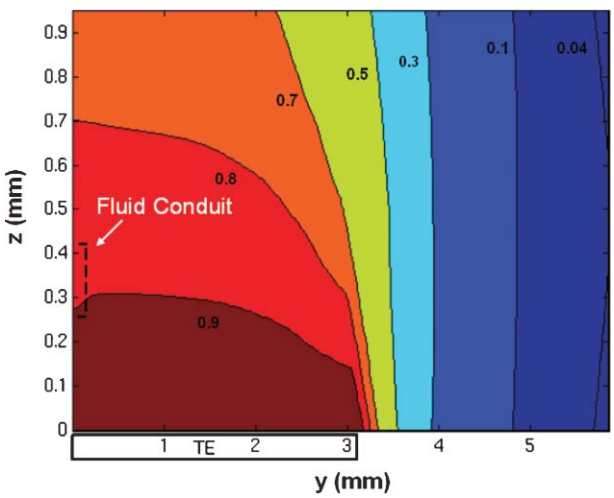

Fig. 7 The steady state, dimensionless temperature $\phi = \left(\frac{T_\infty - T(t)}{T_\infty - T_i(t)}\right)$ distribution and contours in the y–z cross-section located at $x = 0$ in the absence of flow. The power input to the TE unit is $P = 6.9$ W.

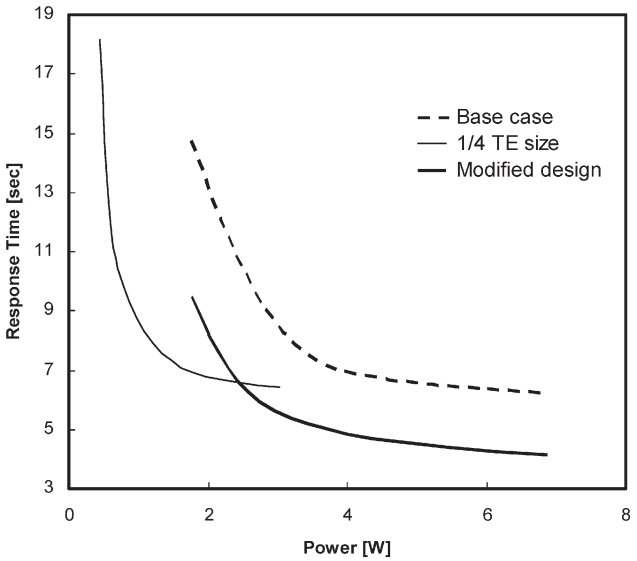

Fig. 8 The simulated response time in the absence of flow as a function of the TE power in the absence (dashed line) and presence (heavy solid line) of the air gap (case I) and reduced TE footprint (light solid line, case II).

In case II, we reduce the footprint of the TE unit to about 1/4 of the base case. We assume that the smaller unit will consume about 1/4 of the power of the unit used in our experiments (base case) and reduce the volume of the chip affected by the cooling. Fig. 8 indicates that the reduction in the footprint area of the thermoelectric unit carries only a small penalty in terms of response time.

5. Examples of applications of the PC valve

The PC valve can be used to control fluid flow in microfluidic systems. It is especially advantageous in systems in which liquid slugs are pneumatically driven. In such cases, the PC valve offers the unique advantage of self-actuation; it allows one to block the liquid flow without the need for a sensor, simply by precooling the conduit section to be blocked. As long as the liquid slug is upstream of the cooled segment, the valve remains open and allows unhindered passage of air. When the liquid slug arrives at the valve location, the liquid freezes, blocking the passage. In contrast to a conventional valve, precise timing of the valve actuation is not necessary. Section 5.1 describes a component for sample metering and distribution that takes advantage of the self-actuated mode of

valve operation. In section 5.2, we describe the use of two ice valves to pressurize a PCR reactor. In experiments with open (un-pressurized) PCR reactors, we experienced significant bubble formation, which adversely affected the PCR amplification efficiency. In the case of the PCR reactor, the valve downstream of the reactor is operated in a self-actuating, precooled mode. Once the sample flow is blocked with the downstream valve, the upstream valve is actuated. Since the fluid is stationary, precise timing of the upstream valve is not critical. Finally, section 5.3 describes the use of the ice valve to fill and empty a closed loop.

5.1 Distribution and metering of liquid samples

Frequently, analytical devices require specific volumes of a fluid sample to be allocated to several analysis paths. Fig. 9 is a photograph of a manifold that divides a sample into four metering chambers. The volume of the metering chambers may be identical or different. The conduits downstream of the metering chambers are precooled with a thermoelectric unit to about −20 °C. As the sample enters through the inlet conduits, it fills the metering chambers, and displaces the air through the outlet conduits.

Fig. 10 depicts the displacement process. The meniscus at the front end of the liquid slug acts as a piston that displaces the air from the metering chamber. The velocity of the slug and the dimensions of the chamber must be optimized to avoid breaking the liquid slug. Slug breakage typically does not occur when the chamber walls are dry prior to introduction of the slug. The filling order depends on the channel size and surface conditions. When the liquid reaches the precooled segments of the exit conduits, it freezes, and the flow in these branches stops. The video *Sample Distribution* that documents the filling process is available in Electronic Supplementary Information†. This application demonstrates the self-actuated operation of the PC valve without the need for a sensor to detect the position of the liquid slug. Consistent with our needs, the valve allows free passage of air and blocks the passage of liquid.

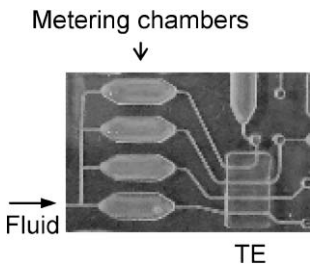

Fig. 9 A photograph of a polycarbonate-based component: the PC valve is used for the distribution and metering of a sample into multiple (four shown) analysis paths.

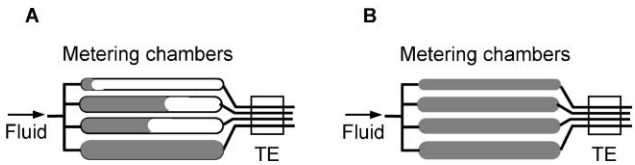

Fig. 10 A schematic description of the displacement process. (**A**) A sample flows into the metering chambers and displaces air; (**B**) the sample fills all the metering chambers and freezes at the location of the phase change valve (TE).

5.2 Stationary PCR

The process of identifying the presence of pathogens often requires PCR amplification of DNA. One mode of achieving chip-based PCR is to hold the reagents in a chamber while cycling the chamber temperature (stationary PCR). One problem often experienced with stationary PCR microreactors is the formation of bubbles. The bubbles may expel the reagents from the PCR chamber, thereby reducing the amplification efficiency. A possible remedy to minimize or eliminate bubble formation is to pressurize the PCR chamber by sealing it. Below, we describe the use of PC valves for this purpose.

Fig. 11A is a photograph of the PCR reactor fabricated with polycarbonate. The PCR mixture is driven into the reaction chamber through the inlet PC valve. During this process, the inlet valve is maintained at room temperature, allowing unhindered passage of the liquid through it. The liquid fills the PCR chamber, displacing the air through the precooled exit valve. Once the air has been displaced out of the chamber and the liquid arrives at the exit valve location, the liquid freezes and blocks the passage. Subsequently, the inlet PC valve is closed. Since at this instant the sample is stationary, the precise closing time of the inlet valve is not critical, and the upstream valve can be programmed in an open loop control mode. The intake (upstream) valve can be replaced with a check valve that allows flow passage only in the downstream direction. Once both the upstream and downstream valves are closed, the temperature of the PCR reactor is cycled.

To demonstrate that such a device can be used in practice, we carried out a successful amplification of 305-bp fragments from *Bacillus cereus* genomic DNA. To avoid carry-over contamination, we used a new polycarbonate-based chip. The inlet and outlet conduits were both 380 μm × 200 μm (width × height). The PCR chamber volume was 10 μL. A control run was carried out in a standard bench-top PCR thermocycler (Techne Incorporated, Princeton, NJ). Both the control and

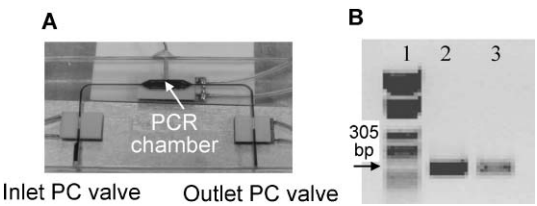

Fig. 11 A PCR chamber equipped with phase change valves to assure pressurized operating conditions that suppress bubble formation. (**A**) A photograph of the polycarbonate-based PCR microdevice; (**B**) Images of ethidium bromide stained DNA products in a 1% agarose gel. Lane 1: marker; lane 2: control from a benchtop thermocycler; and lane 3: product from a polycarbonate based test chip sealed with PC valves.

on-chip PCR were carried out with the same reagents: 50 mM Tris-HCl (pH 9.0), 20 mM $(NH_4)_2SO_4$, 1.5–3.5 mM $MgCl_2$, 200 μM of dNTP, and 0.1 μg μL^{-1} BSA, 1.2 μM and 0.7 μM F- and R-Primers, 6.5 ng μL^{-1} DNA template, and 0.2 U μL^{-1} Taq. The thermal cycling protocol consisted of an initial denaturation at 94 °C for 120 s, 25 cycles (94 °C, 20 s; 55 °C, 20 s; 72 °C, 20 s), and a final extension at 72 °C for 120 s. After the amplification, both the products of the positive control and the chip-based PCR were electrophoresed in 1% agarose gel. Fig. 11B shows the images of ethidium bromide stained DNA products in the gel. Lanes 1, 2, and 3 correspond, respectively to the marker, the control, and the chip-based PCR products. The chip based PCR yielded a visible image of the product, indicating that the PCR reaction successfully occurred with a pair of PC valves.

5.3 Filling and withdrawing samples from a closed loop

In certain applications such as magneto-hydrodynamically (MHD) driven circular chromatography,[21] MHD-driven PCR,[22] MHD stirrer,[23] and self-actuated flow-cycling PCR,[24,25] it is desirable to flow reagents in a closed loop. In a pneumatic system, the filling of the closed loop without creating gas bubbles represents a challenge. The PC valve offers a convenient solution. Fig. 12A depicts a closed flow loop equipped with a PC valve to aid in the filling and withdrawal of a liquid sample. The loop is connected to an inlet conduit and an exit conduit at points **A** and **B**, respectively. The inlet and exit conduits divide the loop into a long arc segment and a short arc segment. The thermoelectric unit is installed to cool part of the shorter arc segment between the inlet and outlet conduits (Fig. 12A). Fig. 12B provides a photograph of the loop fabricated with polycarbonate and equipped with a thermoelectric unit. Figs. 12B–G depict the sequence of steps needed to fill (first row) and empty (second row) the flow loop. Initially, the valve is open. A liquid slug enters through the inlet conduit and fills the short arc segment between the inlet and the exit conduits (Fig. 12B). This is the path of least resistance to the flow. Next, a portion of the liquid slug is frozen (the valve closes), and the liquid must flow through the longer (right) arc (Fig. 12C) until the loop fills entirely with liquid (Fig. 12D). At this instant, the PC valve opens, and the two other valves (not shown here) upstream and downstream of the loop are closed. The sample now can circulate around the loop as many times as desired. To withdraw the sample from the loop, the upstream and downstream valves (not shown) are opened, and the PC valve along the short segment of the loop is closed (Fig. 12E). A gas stream delivered through the inlet conduit (Fig. 12F) displaces the sample (Fig. 12G). A video describing the filling and emptying process is available in Electronic Supplementary Information†.

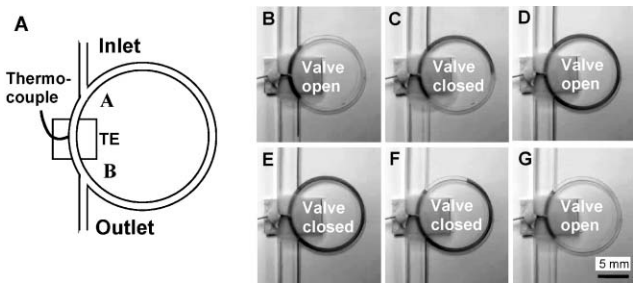

Fig. 12 A PC valve-aided liquid sample introduction into and withdrawal from a closed flow loop (conduit dimensions $W \times H$: 800 μm × 300 μm, loop inner diameter 11.7 mm). (**A**) A schematic depiction of the device. (**B–G**) A sequence of steps for sample filling and withdrawal. (**B**) The PC valve is open, and the sample fills the short segment of the loop between the inlet and exit conduits. (**C**) The PC valve closes, and the sample fills the long section of the loop. (**D**) The valve opens to allow circulation around the loop. (**E**) The valve closes. (**F**) Air displaces the liquid from the long segment of the loop. (**G**) The loop is nearly empty.

6. Conclusions

The thermal actuation, flow control method presented in this paper operates by chilling the flow conduits themselves, and it does not require any moving parts. It is relatively simple to implement, noninvasive, reusable, leakage-free, and electronically addressable. We experimentally characterized the PC valve and found that its response time ranged from 0.5 seconds (under precooled conditions) to about 10 seconds (under high flow conditions and without precooling). In the absence of precooling, the time constant of the valve is mostly dictated by the thermal inertia of the thermoelectric unit. Further improvement in performance can be obtained by inserting the microfluidic device into a refrigerated chamber and by enhancing ice nucleation to increase the supercooling temperature.

Using finite elements modeling, we simulated the valve performance and predicted the valve response time as a function of operating conditions and chip design. The model predictions are in good agreement with experimental observations.

In the preferred mode of operation, the valve works in a self-actuated mode, *i.e.*, a pre-chilled conduit segment allows the free passage of displaced air and freezes the liquid when it arrives at the valve location. A number of examples of applications were described such as sample distribution and metering, bubble-free PCR amplification, and the filling of a closed loop.

For the valve to be effective, the freezing point of the working liquid must not be too low. There is also a concern that the repetitive freezing and thawing may adversely affect biomaterials. Issues of biocompatibility will require further studies. We note, however, that, in most cases, only a fraction of the working fluid will be subjected to freezing and thawing. Furthermore, it appears that the phase change valve did not have any adverse effect on the PCR amplification process.

Acknowledgements

We are grateful to Drs D. Malamud, W.R. Abrams, Z. Wu, and M. G. Mauk, and Ms C. Davis and Mr G. Tong (University of Pennsylvania) and P. Corstjens (Leiden University) for helpful discussions and Mr M. Tao (Thomas Jefferson High School of Science and Technology) for

assistance in the characterization experiments. The experimental work was supported, in part, by NIH grant U01DE014964 to the University of Pennsylvania.

References

1 T. Vilkner, D. Janasek and A. Manz, Micro Total Analysis Systems, Recent Developments, *Anal. Chem.*, 2004, **76**, 3373–3386.
2 A. Baldi, Y. D. Gu, P. E. Loftness, R.A. Siegel and B. Ziaie, A Hydrogel-Actuated Environmentally Sensitive Microvalve for Active Flow Control, *J. Microelectromech. Syst.*, 2003, **12**, 613–621.
3 S. Lee, W. Jeong and D. J. Beebe, Microfluidic Valve with Cored Glass Microneedle for Microinjection, *Lab Chip*, 2003, **3**, 164–167.
4 D. T. Eddington, R. H. Liu, J. S. Moore and D. J. Beebe, An Organic Self-Regulating Microfluidic System, *Lab Chip*, 2001, **1**, 96–99.
5 P. Griss, H. Andersson and G. Stemme, Expandable Microspheres for the Handling of Liquids, *Lab Chip*, 2002, **2**, 117–120.
6 T. Rogge, Z. Rummler and W. K. Schomburg, Polymer Micro Valve with a Hydraulic Piezo-Drive Fabricated by The AMANDA Process, *Sens. Actuators, A*, 2004, **110**, 206–212.
7 A. Terray, J. Oakey and D. W. M. Marr, Microfluidic Control Using Colloidal Devices, *Science*, 2002, **296**, 1841–1844.
8 H. Hartshorne, C. J. Backhouse and W. E. Lee, Ferrofluid-Based Microchip Pump and Valve, *Sens. Actuators, B*, 2004, **99**, 592–600.
9 M. A. Unger, H. P. Chou, T. Thorsen, A. Scherer and S. R. Quake, Monolithic Microfabricated Valves and Pumps by Multiplayer Soft Lithography, *Science*, 2000, **288**, 113–116.
10 J. S. Go and S. Shoji, A Disposable, Dead Volume-Free and Leak-Free in-Plane PDMS Microvalve, *Sens. Actuators, A*, 2004, **114**, 438–444.
11 D. J. Beebe, J. S. Moore, J. M. Bauer, Q. Yu, R. H. Liu, C. Devadoss and B. H. Jo, Functional Hydrogel Structures for Autonomous Flow Control Inside Microfluidic Channels, *Nature*, 2000, **404**, 588–590.
12 Q. Luo, S. Mutlu, Y. B. Gianchandani, F. Svec and J. M. J. Fréchet, Monolithic Valves for Microfluidic Chips Based on Thermoresponsive Polymer Gels, *Electrophoresis*, 2003, **24**, 3694–3702.
13 R. H. Liu, J. Bonanno, J. N. Yang, R. Lenigk and P. Grodzinski, Single-Use, Thermally Actuated Paraffin Valves for Microfluidic Applications, *Sens. Actuators, B*, 2004, **98**, 328–336.
14 R. Pal, M. Yang, B. N. Johnson, D. T. Burke and M. A. Burns, Phase Change Microvalve for Integrated Devices, *Anal. Chem.*, 2004, **76**, 3740–3748.
15 C. D. Bevan and I. M. Mutton, Freeze-Thaw Flow Management: A Novel Concept for High-Performance Liquid Chromatography, Capillary Electrophoresis, Electrochromatography and Associated Techniques, *J. Chromatogr., A*, 1995, **697**, 541–548.
16 Y. He, Y. H. Zhang and E. S. Yeung, Capillary-Based Fully Integrated and Automated System for Nanoliter Polymerase Chain Reaction Analysis Directly From Cheek Cells, *J. Chromatogr., A*, 2001, **924**, 271–284.
17 J. Liu and L. Gui, Ice valve for a Mini/Micro Flow Channel, *J. Micromech. Microeng.*, 2004, **14**, 242–246.
18 Z. Chen, P. L. A. M. Corstjens, M. Zuiderwijk, J. Wang, M. G. Mauk, H. H. Bau, W. R. Abrams and D. Malamud, Phosphor Reporter Particle-Based Disposable Device for the Rapid Detection of HIV at the Point of Care, accepted for presentation in the μTAS 2005, Boston, Massachusetts, USA, October 9th–13th, 2005.
19 http://www.matweb.com.
20 F. M. White, *Viscous Fluid Flow*, McGraw-Hill, New York, 1974, p. 123.
21 J. C. T. Eijkel, C. Dalton, C. J. Hayden, J. P. H. Burt and A. Manz, A Circular AC Magnetohydrodynamic Micropump for Chromatographic Applications, *Sens. Actuators, B*, 2003, **92**, 215–221.
22 J. West, B. Karamata, B. Lillis, J. P. Gleeson, J. Alderman, J. K. Collins, W. Lane, A. Mathewson and H. Berney, Application of Magnetohydrodynamic Actuation to Continuous Flow Chemistry, *Lab Chip*, 2002, **2**, 224–230.
23 J. P. Gleeson, O. M. Roche, J. West and A. Geb, Modeling Annular Micromixers, *SIAM J. Appl. Math.*, 2004, **64**, 1294–1310.
24 Z. Chen, S. Qian, W. R. Abrams, D. Malamud and H. H. Bau, Thermosiphon–Based PCR Reactor: Experiment and Modeling, *Anal. Chem.*, 2004, **76**, 3707–3715.
25 E. K. Wheeler, W. Benett, P. Stratton, J. Richards, A. Chen, A. Christian, K. D. Ness, J. Ortega, L. G. Li, T. H. Weisgraber, K. Goodson and F. Milanovich, Convectively Driven Polymerase Chain Reaction Thermal Cycler, *Anal. Chem.*, 2004, **76**, 4011–4016.